

2012

Designated vs Non-designated Areas for Condenser Subcooling

Gustavo Pottker
gpottker@illinois.edu

Predrag S. Hrnjak

Follow this and additional works at: <http://docs.lib.purdue.edu/iracc>

Pottker, Gustavo and Hrnjak, Predrag S., "Designated vs Non-designated Areas for Condenser Subcooling" (2012). *International Refrigeration and Air Conditioning Conference*. Paper 1332.
<http://docs.lib.purdue.edu/iracc/1332>

This document has been made available through Purdue e-Pubs, a service of the Purdue University Libraries. Please contact epubs@purdue.edu for additional information.

Complete proceedings may be acquired in print and on CD-ROM directly from the Ray W. Herrick Laboratories at <https://engineering.purdue.edu/Herrick/Events/orderlit.html>

Designated vs. Non-Designated Areas for Condenser Subcooling

Gustavo POTTKER¹, Pega HRNJAK^{1*}

¹Department of Mechanical Science and Engineering
University of Illinois at Urbana-Champaign
1206 West Green Street, Urbana, IL 61801, USA

* Corresponding Author: pega@illinois.edu

ABSTRACT

The difference in effect of subcooling in a condenser (non-designated area, NDA) vs. in a subcooler (designated area of the same condenser, DA) on the system performance is experimentally analyzed in a vehicular air conditioning system operating with R134a and R1234yf. With a unique set of microchannel condensers, an experimental comparison between subcooling generated in non-designated area (NDA) and designated area (DA) of the condenser showed that both configurations yielded similar values of maximum COP improvement within the operating conditions considered. The results suggested that the way condenser subcooling is achieved, either in a DA or a NDA, may not be important in terms of COP. The experimental results for non-designated subcooling indicated that the larger the air-refrigerant temperature difference in the condenser, due to a large cooling capacity needed for a given condenser size, the higher the COP maximizing subcooling and the maximum COP improvement from condenser subcooling. For R1234yf, as the temperature difference in the condenser increased from 12°C to 28°C, the COP maximizing subcooling increased from 6°C to 16°C and the COP gains, from 6% to 44%. Experimental and numerical results also demonstrated that condensers with a higher air-refrigerant temperature difference in the condenser would require a larger COP maximizing area ratio allocated for subcooling. Nevertheless, a fixed designated area yielded near maximum COPs within a reasonable range of operating conditions.

1. INTRODUCTION

Pottker and Hrnjak (2012) have numerically and experimentally demonstrated that, as the condenser subcooling is increased, the COP reaches a maximum as a result of a trade-off between increasing refrigerating effect (by Δq , Figure 1), due to a reduction of the condenser exit refrigerant temperature (by $\Delta T_{c,out}$, Figure 1), and increasing specific compression work (by Δw , Figure 1), due to an increase in condensing pressure (by $\Delta T_{c,sat}$, Figure 1). Condenser subcooling can be achieved in various ways but in this paper the authors are focused on the trade-off between allocation of certain areas of the heat exchanger for subcooling or for condensing function. Subcooling in a so-called non-designated occurs naturally in the condenser, typically envisioned after the liquid-vapor interface is eliminated inside the condenser as liquid accumulates towards the exit of the heat exchanger.

The effect of subcooling is typically seen during a refrigerant charge procedure as shown schematically in Figure 2, for a typical air conditioning system equipped with a 2-pass cross-flow condenser and a thermostatic expansion valve (TXV). The majority of the refrigerant mass added to such a system accumulates in the form of liquid in the condenser, increasing the subcooling, while a small portion stays in the evaporator as inlet quality decreases.

Condenser subcooling can also be generated in a so-called designated area when a liquid receiver is installed before the last pass of the condenser, as illustrated by Figure 3. As refrigerant charge is added, the subcooled liquid first fills the last pass, between points A and B (Figure 3). After point B, liquid begins to accumulate in the receiver and the condenser subcooling becomes fixed in the designated area, between points B and C. Such air-conditioning (AC) systems are normally designed to operate within this region, usually denominated “operating plateau”. Pomme, (1999) and Abraham *et al.* (2006) provided similar descriptions and, supported by experimental data. Condensers

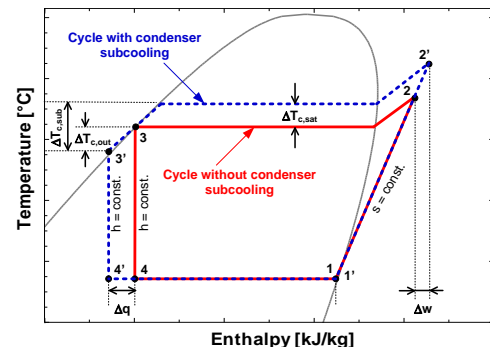


Figure 1: Comparison between theoretical cycles with and without condenser subcooling

with a designated area for subcooling are typically used in state-of-the-art automotive AC systems equipped with an integrated receiver, as described by Yamanaka *et al.* (1997) and Ravikumar and Karwall (2005). The receiver is used to store extra mass of refrigerant needed to meet high cooling load conditions and compensate for refrigerant leakages (Abraham *et al.*, 2006).

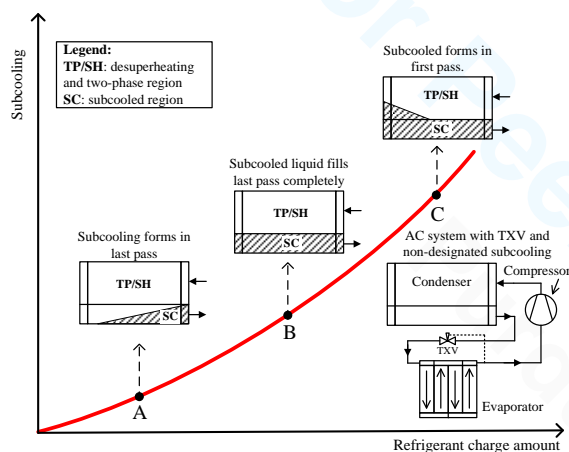


Figure 2: Typical variation of the subcooling with the refrigerant charge in a non-designated area

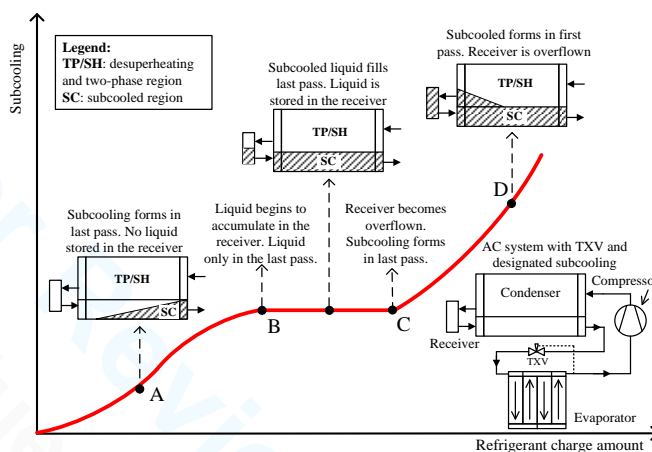


Figure 3: Typical variation of the subcooling with the refrigerant charge in a designated area

In the non-designated subcooling configuration (Figure 2), the condenser subcooling can be used to maximize COP for the design condition as shown by Pottker and Hrnjak (2012), but subcooling may turn out to be excessive (system overcharged) or insufficient (system undercharged) in off-design operating conditions. This could be specially an issue in variable speed systems, where variations of the cooling capacity affect the temperature difference between air and saturated refrigerant in the condenser and consequently the room for subcooling. In the designated subcooling approach (Figure 3), as long as liquid is accumulated in the receiver, subcooled liquid will always be present at the condenser exit. However, a fixed subcooling area does not necessarily guarantee that the system will operate under a COP maximizing subcooling in all operating conditions. In case of microchannel cross-flow condensers, differences may also regard refrigerant distribution in the parallel channels connected by the header. Infrared images of a microchannel condenser with non-designated subcooling taken by Pottker and Hrnjak (2012) revealed mal-distribution of liquid in the last pass which could potentially affect the condenser performance. In the designated subcooling, however, the subcooling pass would not be subject to such issue if liquid is completely separated from vapor in the receiver.

One of the objectives of this paper is to investigate whether the way the subcooling is achieved affects the system performance in terms of COP. To do so, the performance of a system configuration in which the subcooling is generated in a non-designated area is experimentally compared to that of an almost identical configuration in which subcooling is achieved in a designated area. To the best of the authors' knowledge there is not such experimental study in the open literature. Another point to be addressed is whether the control of the condenser subcooling in order to maximize COP, as suggested by Pomme (1999) and Strupp *et al.* (2010), would be worth it or a fixed subcooling area would be able to keep the system near COP maximizing subcooling values within a given range of operating conditions. Before doing so, this study will examine the effect of the air-refrigerant temperature difference in the condenser on the COP maximum gains due to subcooling, based on experimental data with R134a and R1234yf.

2. EXPERIMENTAL METHODS

The experimental system under investigation is a modified 2007 production line R134a automotive AC system. The compressor is a piston-displacement with a fixed swept volume of 214 cm³/REV connected through the same shaft to an electrical driving motor with variable speed capabilities. The original evaporator, a plate-and-fin type, was maintained together with the original heating ventilation air conditioning (HVAC) module. The condensers used are all parallel cross-flow microchannel heat exchangers with a single-slab, face area of 0.24 m², core depth of 16 mm, fin density of 18 louvered fins per inch and a total of 39 parallel microchannels tubes. Figure 4 shows the system configurations with and without a designated area for subcooling.

In the non-designated subcooling (Figure 4, left), the subcooling was varied by adding refrigerant mass in increments after the receiver was completely filled with liquid so that subcooled refrigerant would accumulate towards the condenser exit. The non-designated subcooling condenser, named condenser #0, has two passes as shown in Table 1. For the experiments with designated area for subcooling (Figure 4, right), five almost identical condensers with different pass arrangements were used, including condenser #0.

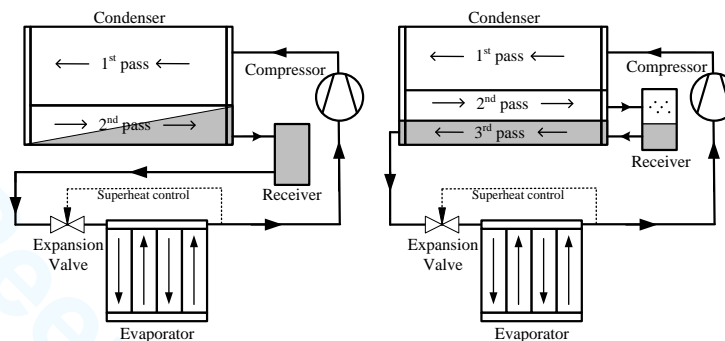


Figure 4: System setups for subcooling obtained in a non-designated (left) and a designated area (right) of the condenser

The heat exchangers were all made by the same manufacturer and have the equal air and refrigerant side characteristics except for the number of channels in the last pass (subcooling pass) which varies: zero (no subcooling pass), 3, 6, 9 and 12 channels as shown in Table 1. The total number of channels, however, is fixed (39 channels).

Therefore, the ratio (DA_{SUB}) between the area allocated for subcooling and the total heat exchanger area is varied from 0% to 30% (Table 1). By changing the DA_{SUB} , the subcooling is varied while the receiver was maintained approximately half full with liquid. The design is made so that in the condensing part of the heat exchanger the ratio between the number of tubes in the first and in the second pass is always equal to two.

Table 1: Pass arrangement of the condensers

	Number of microchannels			DA_{SUB}
	1 st Pass	2 nd Pass	3 rd	
Condenser #0	26	13	0	0%
Condenser #3	24	12	3	8%
Condenser #6	22	11	6	15%
Condenser #9	20	10	9	23%
Condenser #12	18	9	12	31%

The experimental facility comprises the two environmental chambers and the refrigeration circuit. The condenser was installed at the inlet of an open-loop wind tunnel inside the outdoor chamber. The evaporator together with HVAC module was attached to the open-loop wind tunnel of the indoor chamber. In both chambers, a set of PID-controlled electrical heaters were used to control the air inlet temperature to the heat exchangers. In the outdoor chamber, an external chilled water coil removed the energy dissipated by condenser and electrical heaters. A dehumidifier was able to keep dew-point temperatures low enough for fully dry-conditions in the evaporator. The air flow rates were controlled with variable speed blowers. Air-side pressure drop across the flow nozzles was measured by differential pressure transducers while Type-T thermocouples measured the dry-bulb air temperature at the nozzle exits, in order to obtain the air flow rates. T-type thermocouple grids were installed upstream and downstream of evaporator and condenser to measure the dry-bulb temperatures. In the evaporator wind-tunnel, chilled-mirror dew-point sensors were also installed. Type-T immersed thermocouples and absolute pressure transducers were conveniently placed throughout the refrigeration circuit. In order to measure refrigerant mass flow rate, a Coriolis-type mass flow meter was installed between the liquid receiver and the expansion valve.

The calculated air flow rate combined with dry-bulb and dew-point temperature readings were used to obtain the cooling capacity on the air side of the evaporator. In addition, the cooling capacity was independently obtained by an energy balance on the refrigerant side, using mass flow rate and enthalpies obtained from pressure and temperature readings. The compressor power was obtained using measurements from a torque transducer and a tachometer mounted in the shaft that connects the compressor to the electrical motor. An uncertainty propagation analysis carried out in EES (2007) revealed an experimental uncertainty of $\pm 6\%$ for the cooling capacity obtained from the air-side, $\pm 3\%$ for that obtained from the refrigerant side and $\pm 5\%$ for the COP calculated with the cooling capacity on the refrigerant-side. Air and refrigerant side cooling capacities agreed within $\pm 3\%$.

3. COMBINED EFFECT OF AIR-REFRIGERANT TEMPERATURE DIFFERENCE AND CONDENSER SUBCOOLING GENERATED IN A NON-DESIGNATED AREA

It is almost intuitive that the temperature difference between the inlet air and the condensing refrigerant can affect the subcooling in the condenser. The larger this temperature difference, in theory, the greater the room for subcooling the liquid in the condenser. For a given resistance to heat transfer, a higher air-refrigerant temperature difference in the condenser can be the result of a larger heat transfer rate. For instance, a given air-cooled AC system with heat exchangers of fixed air-dominant resistance to heat transfer may be subject to different cooling loads

depending on the operating conditions. In case of variable speed systems, the compressor speed may be increased to raise the cooling capacity and match the cooling demand. As a consequence, heat transfer rate in the condenser will increase as well as the air-refrigerant temperature difference. On the other hand, for a given condenser heat transfer load, a higher resistance to heat transfer also yields a larger air-refrigerant temperature difference. It is known that, especially due to space constraints, automotive AC condensers typically have smaller heat transfer areas per unit of cooling capacity than those of stationary, commercial or industrial applications.

In order to investigate the effect of the air-refrigerant temperature difference in the condenser on the COP benefits due to subcooling, the AC system with the condenser of non-designated area for subcooling was tested at three different cooling capacity settings, i.e. low, medium and high, as shown in Table 2. By changing the cooling capacity, the heat transfer rate in the condenser is also varied and, as a result, the air-refrigerant temperature difference in the condenser is changed since air-side heat transfer area and air inlet conditions are kept constant.

Variations of refrigerant-side heat transfer coefficient are negligible since the air-side resistance is dominant in the condenser. Table 2 shows that the cooling load was changed by varying both the air inlet temperature and face velocity of the evaporator, while air inlet temperature and face velocity of the condenser were kept constant.

Table 2: Test conditions

Capacity setting	T_{outdoor}	T_{indoor}	$V_{f,e}$	$V_{f,c}$	Q_{cooling}
	[°C]	[°C]	[m/s]	[m/s]	[kW]
Low	35.0	25.0	2.0	1.5	2.6
Medium	35.0	30.0	2.6	1.5	4.1
High	35.0	35.0	3.0	1.5	5.3

At each cooling capacity, in order for COP to be the only measure of improvement as subcooling was varied, the evaporator heat transfer rate on the air-side was matched within $\pm 0.3\%$ by manipulating the compressor speed accordingly. The condenser subcooling was varied in small increments by adding refrigerant charge while the evaporator exit superheat was kept at 10°C by manipulating the expansion valve opening. Two different refrigerants were tested in the same system and under the same operating conditions: R134a and R1234yf.

Figs. 5 and 6 show results for normalized COP, inlet saturation temperature and exit temperature of the refrigerant as a function of the condenser subcooling for high, medium and low cooling capacities with R134a. The continuous lines in the charts indicate a curve fitting of the experimental points.

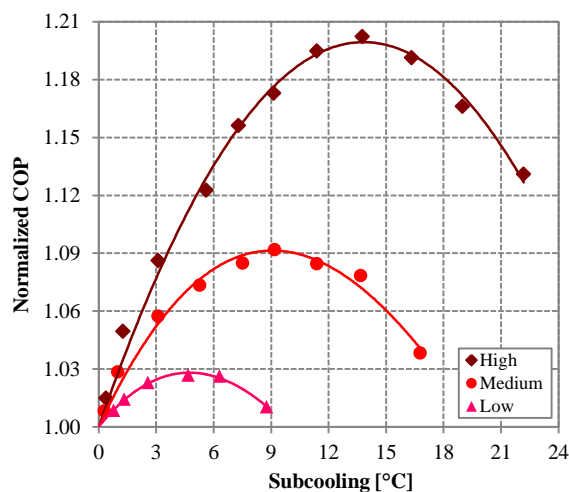


Figure 5: Normalized COP as a function of the condenser subcooling for high, medium and low cooling capacities (R134a)

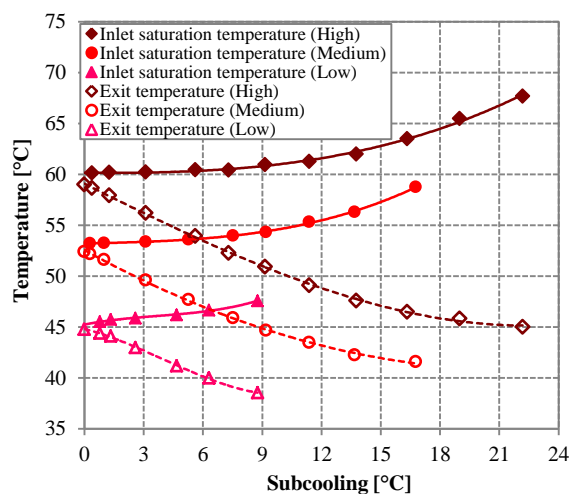


Figure 6: Inlet saturation temperature and exit temperature of the refrigerant as a function of the condenser subcooling for high, medium and low cooling capacities (R134a)

According to Figure 5, regardless the cooling load, the COP reaches a maximum as the subcooling is increased. In other words, the system efficiency was improved by the subcooling, relative to baseline condition without subcooling, for all cooling loads. As mentioned by Potker and Hrnjak (2012), the maximum COP is primarily a result of a trade-off between increasing evaporator enthalpy difference, due to the decrease of the refrigerant temperature at the condenser exit (Figure 6), and increasing specific compression work, due to an increase in the saturation temperature (Figure 6), although secondary factors may also be important.

Figure 5 demonstrates that the COP maximizing subcooling increases with the cooling load. At the high cooling load, the COP maximizing subcooling is around 14°C , while for medium and low loads it decreases to 9°C and 5°C , respectively. Likewise, one could also say that the COP maximizing subcooling increases with the reduction of the size of the condenser relative to its heat transfer rate. At higher cooling loads, the heat rejection rate is greater,

leading to a higher temperature difference between inlet air (at 35°C) and saturated refrigerant in the condenser, as seen in Figure 6. A larger air-refrigerant temperature difference provides a greater room for subcooling in the condenser, subsequently leading to an increase of the COP maximizing subcooling. Under the perspective of the Second Law of Thermodynamics, throttling losses are larger when the air-refrigerant temperature difference is higher. Since subcooling aims to reduce the refrigerant temperature at the condenser exit and consequently the throttling losses, one could think that a higher subcooling would be more welcome in such operating conditions. COP gains are affected by evaporator enthalpy difference (Δh_{evap}), isentropic specific work ($\Delta h_{\text{is,cp}}$) and isentropic efficiency, with help from the Eq. 1.

$$COP = \eta_{\text{is,cp}} \frac{\Delta h_e}{\Delta h_{\text{is,cp}}} \quad (1)$$

From Figure 5, it can be observed that the higher the cooling load, the higher the maximum COP improvement. For the high load, COP increases up to 20% while for medium and low loads maximum improvements were about 9% and 3%, respectively. In terms of relative size of the heat exchanger, these results indicate that applications where the size or overall heat transfer coefficient of the condenser is smaller relative to the heat transfer rate would tend to benefit more from condenser subcooling. Since the COP maximizing subcooling is higher for larger cooling loads, a greater reduction of the refrigerant temperature at condenser exit takes place until the system reaches the maximum COP, as seen in Figure 6. From zero to COP maximizing subcooling, the refrigerant temperature at the condenser exit reduces by 11.4°C at the high load, against 7.7°C and 3.6°C for medium and low loads, respectively. A larger temperature drop at the condenser exit yields a greater relative gain in refrigerating effect, which has been shown by Pottker and Hrnjak (2012) to be the dominant effect to determine maximum COP gains due to subcooling. The same authors also demonstrated that the increase of the temperature lift, due to the rise in the condensing temperature, can also increase relative gain in refrigerating effect. For high, medium and low loads, the relative increase in refrigerating effect was equal to 14%, 9% and 4%, respectively, at maximum COP conditions which mostly explains the higher COP gains obtained at higher cooling capacities (see Eq. 1). The changes in the isentropic compression work due to subcooling play a minor role towards the maximum COP improvements.

The COP improvements are also affected by changes in the isentropic efficiency of the compressor. Between zero and COP maximizing subcooling, the isentropic efficiency increased 5% and 1% for high and medium loads, respectively, due to the effect of lower compressor speeds to match the cooling capacity as subcooling was increased. At the low load, however, the isentropic efficiency actually decreased, most likely due to operation at lower than designed compressor speeds. Figure 7 shows infrared images taken at the condenser inlet surface at COP maximizing subcooling conditions for each cooling capacity setting. The dashed lines are an attempt to indicate the subcooling zone. As cooling load increases, the size of the condenser relative to its heat transfer rate is smaller. As a result, one could think that, in order to maximize COP, less area should be taken from the condensing zone to accommodate the subcooling region. The images, however, suggest the opposite. It can be seen that the higher the cooling capacity, the larger the subcooling area needed to maximize COP. In other words, at higher loads more area should be allocated to subcool liquid in order to maximize COP. Figure 8 shows the normalized COP as a function of the condenser subcooling for high, medium and low cooling capacities with R1234yf.

For the high condition, the COP near zero subcooling was not measured due to constraints of the system and had to be estimated based on an extrapolation of the experimental data at neighboring subcooling values. When compared to R134a results, similar conclusions can be drawn for R1234yf. The COP was improved by the subcooling for all cooling loads. Like R134a, for R1234yf the larger the cooling capacity the higher the COP maximizing subcooling and maximum COP improvement. For the high load, COP increases up to 44% (estimated by extrapolation) while

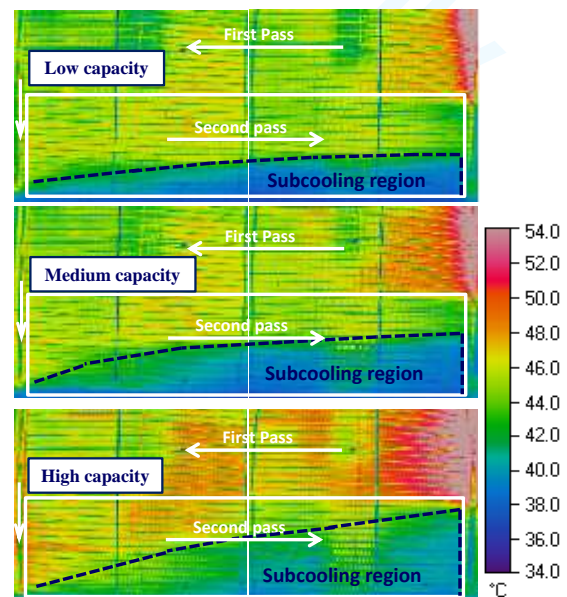


Figure 7: Infrared images taken at the inlet surface of the condenser at COP maximizing subcooling for high, medium and low cooling capacities. Dashed lines indicate approximately the area occupied by the subcooled liquid.

for medium and low loads maximum improvements were about 18% and 6%, respectively. COP improvements are larger for R1234yf than for R134a due to the effect of refrigerant properties, such as latent heat of vaporization, as pointed out by Pottker and Hrnjak (2012).

Figure 9 shows COP maximizing subcooling and normalized maximum COP (with respect to COP at zero subcooling for the given cooling capacity, as in Figs. 5 and 8) as a function of the temperature difference between inlet air (outdoor) and condensing refrigerant obtained at maximized COP conditions, for R134a and R1234yf. For both variables, a curve fitting is suggested with an extrapolation towards no COP improvement and zero COP maximizing subcooling when the temperature difference is zero. This is due to the fact that no subcooling would be possible if the saturation temperature was equal to the air inlet temperature (infinite air flow rate and size of condenser). It can be observed that, although the COP maximizing subcooling is very sensitive to the temperature difference in the condenser, it does not appear to be a function of the refrigerant choice for this heat exchanger. The normalized maximum COP is, however, dependable on the refrigerant choice for the same temperature difference. Similar conclusions have been drawn in a numerical investigation carried out by Pottker and Hrnjak (2012).

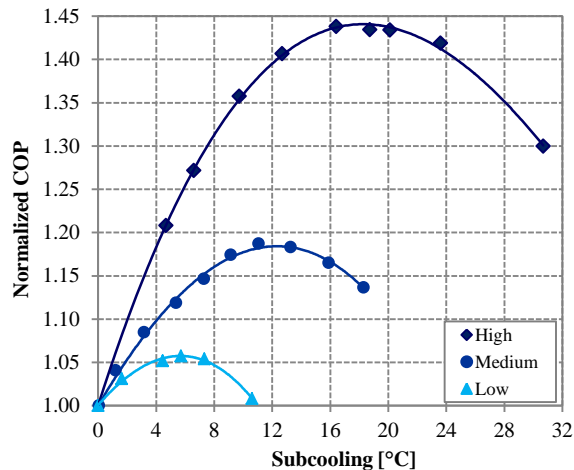


Figure 8: Normalized COP as a function of the condenser subcooling for high, medium and low cooling capacities (R1234yf)

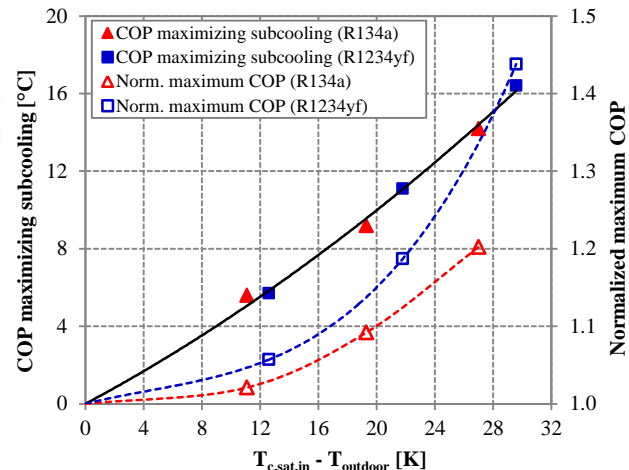


Figure 9: COP maximizing subcooling and normalized maximum COP (with respect to COP at zero subcooling) as a function of the temperature difference between outdoor and condensing refrigerant at maximized COP conditions, for R134a and R1234yf.

4. CONDENSER SUBCOOLING GENERATED IN A DESIGNATED AREA AND COMPARISON WITH NON-DESIGNATED SUBCOOLING

In this section, the performance of the system in which the subcooling is achieved in a non-designated (Figure 4, left) area of the condenser is compared to that of an almost identical system configuration in which subcooling was obtained in a designated area (Figure 4, right). First, the results for system with designated area for subcooling are discussed. For the experiments with designated area, five near identical condensers with different number of channels allocated in the subcooling (last) pass were used (Table 1).

Figure 10 shows the normalized COP and condenser subcooling as a function of DA_{SUB} which is equal to the number of channels allocated for the subcooling divided by the total number of channels, as in Table 1. The dashed lines indicate a curve fitting of the experimental points. The cooling capacity was maintained constant within $\pm 0.5\%$ for each cooling load setting. According to Figure 10, as the area ratio designated for subcooling (DA_{SUB}) increases, the condenser subcooling values become higher for a given cooling load. In addition, for a DA_{SUB} , the subcooling is higher at larger cooling loads, due to higher temperature difference between air and refrigerant in the condenser. It has been previously discussed that the system COP undergoes a maximum as subcooling is increased (Figure 5) and the results for the system with a designated area for subcooling (Figure 10) follow the same trend.

Figure 10 also reveals that the higher the cooling capacity, the larger the COP maximizing area (DA_{SUB}) for subcooling. At the high load, the curve fitting indicates a COP maximizing DA_{SUB} of about 18%, while for medium and low loads the optimum values are equal to 15% and 8%, respectively. Indeed, infrared images from the condenser with non-designated subcooling (Figure 7) indicated similar trends. In addition, these results confirm that a fixed DA_{SUB} does not guarantee that the system will operate at COP maximizing subcooling conditions at different

cooling loads. On the other hand, a fixed designated area of 15% (6 out of 39 channels) would maximize COP for the medium load but also maintain this system near COP maximized conditions for high and low cooling loads, with less than 1% difference from their actual maximum values. Therefore, one could also conclude that, since a fixed DA_{SUB} would yield near maximized subcooling for the three cooling loads, an active control of the subcooling to maximize COP in a non-designated setup would not be worth it for this system under the operating conditions considered.

Figure 11 shows the normalized COP as a function of the subcooling obtained with DA and NDA condensers, for high, medium and low cooling loads. Each of the five subcooling values for the DA setup represents a different condenser (0%, 8%, 15%, 23% and 31% of DA_{SUB}) whereas for the NDA case, all subcooling values were all obtained from the same condenser (Condenser #0, see Table 1) by varying the refrigerant charge. NDA and DA cases are, however, normalized relative to same COP at zero subcooling obtained with the condenser#0.

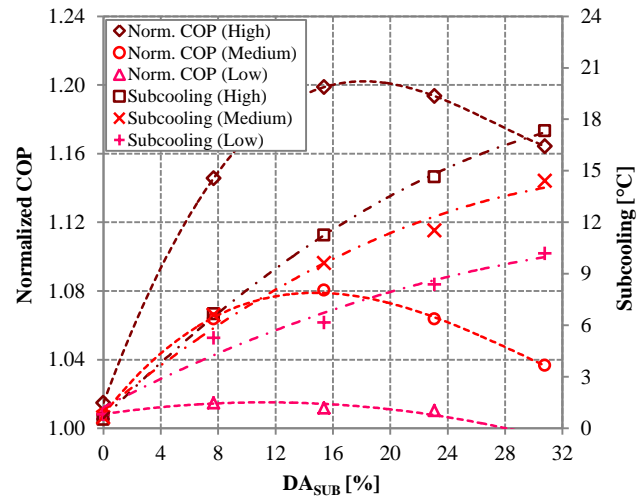


Figure 10: Normalized COP and condenser subcooling as a function of the ratio between the subcooling designated area ratio for high, medium and low cooling loads (R134a).

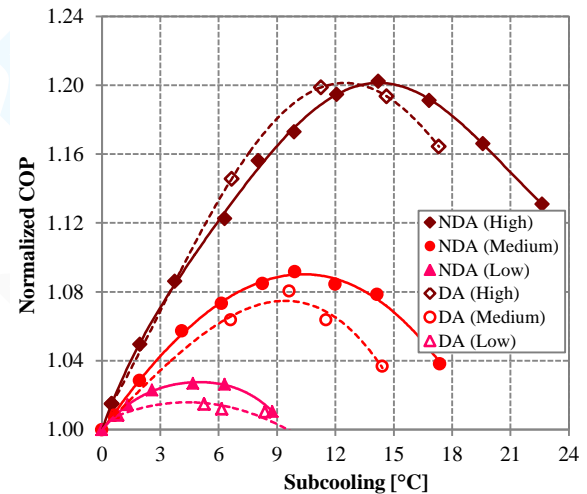


Figure 11: Normalized COP as a function of the condenser subcooling for designated (DA) and non-designated subcooling (NDA), at high, medium and low cooling loads (R134a).

According to Figure 11, both NDA and DA configurations yielded similar values of maximum COP improvement for all cooling loads, with differences of less 1.5%. Besides small deviations, it can be concluded from Figure 11 that the way (DA or NDA) subcooling is achieved may not be important to this system performance in terms of maximum COP. At higher values of subcooling, however, deviations between the performances of the two configurations seem to be more noticeable. Regarding COP maximizing subcooling, NDA and DA configurations resulted in similar values for medium and low loads and were about 3°C apart at the high cooling capacity.

Figure 12 shows infrared images taken at the frontal surface of the NDA (condenser#0) and DA (condenser#6) condensers, respectively, both at the same subcooling of 10°C, for the medium cooling load. Figure 12 suggests that the area occupied by subcooled liquid is approximately the same size for both heat exchangers. In addition, the infrared images show both NDA and DA condensers are subject of mal-distribution of liquid. The mal-distribution is characterized by a non-uniformity of surface temperature among the channels of a same pass. For the NDA condenser this non-uniformity appears throughout the entire second pass, where the bottom channels are at a lower temperature than the upper channels. This may be due liquid pooling in the bottom of the inlet header of the second pass, which would cause the lower channels to be fed with lower quality two-phase flow than that of inlet flow of the upper channels. For the DA condenser, the non-uniformity appears mostly in the right half of the second pass, where it can be seen that the three bottom most channels have a lower temperature than the rest of the channels of the same pass.

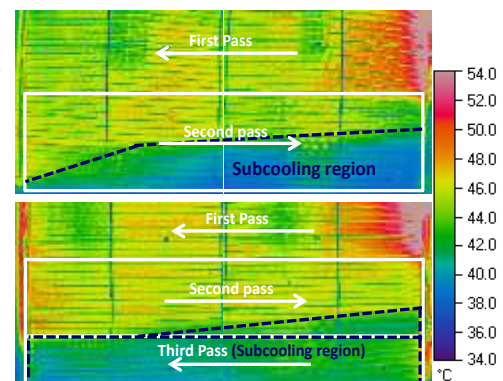


Figure 12: Infrared images from the inlet surface of NDA (top) and DA (bottom) condensers at a subcooling of 10°C for the medium cooling load. Dashed lines to indicate approximately the area occupied by the subcooled liquid.

The fact that DA and NDA condensers presented similar areas occupied by subcooled liquid at the same value of subcooling and both were subject to mal-distribution issues help to explain why they yielded similar maximum performances.

5. NUMERICAL ANALYSIS BASED ON R1234yf

A semi-empirical system model was developed to further elaborate on the combined effect of the condenser subcooling and air-refrigerant temperature difference on the system performance and try to confirm experimentally observed trends. The refrigerant was R1234yf. The model was developed so that compressor, evaporator and connecting lines were treated either with input of experimental data or coefficients regressed from the experimental results. Since the focus is on the subcooling, the condenser was the only component comprehensively modeled with a finite-volume approach, independent of the experimental data. The evaporator was modeled using a fixed average evaporator effectiveness of 74%, obtained from the experimental data at the three cooling capacities. Deviations of the average value with respect to the actual values are within $\pm 2\%$. For the suction line and evaporator refrigerant-side pressure drops, an average experimental frictional pressure drop coefficient was determined. Predicted pressure drop values agreed within $\pm 5\%$ with the experimental data. Suction line was assumed adiabatic and pressure drop along the other connecting lines were neglected. For the compressor, experimentally obtained values of isentropic efficiency for each data point were applied directly as inputs to predict the compressor input power through the model. The condenser was modeled comprehensively with a finite volume method. Each of the two passes of the condenser#0 was divided into 25 volumes. Each finite volume contained the total number of tubes of the respective pass, since the refrigerant distribution in the headers was considered homogeneous. On the air side, uniform inlet temperature and velocity were also assumed. For each finite volume, the heat transfer rate and the outlet enthalpy were calculated using the effectiveness-NTU method for a cross-flow heat exchanger in which the two fluids were unmixed.

In order to determine the “UA” value of each finite volume, only refrigerant and air side convection resistances were considered. The fin efficiency was calculated according to Incropera et al. (2006). The refrigerant and air side heat transfer correlations are indicated in Table 3. The refrigerant-side pressure drop in each finite volume was calculated from widely used friction factor correlations (Table 3) for major losses, while minor losses were neglected. Typical input variables of the model are condenser geometric parameters, inlet air temperature and velocity to the heat exchangers, refrigerant superheat at the evaporator outlet and subcooling at the condenser outlet as well as the system cooling capacity.

Typical outcomes of the model are evaporator and condenser saturation temperature, refrigerant temperature at the condenser exit and COP. Figure 13 shows results of the experimental validation of the model for the normalized COP with respect to its maximum value at the given capacity. The lines represent the numerical results. According to Figure 13, the model was able to capture well the effect of subcooling on normalized COP for all three cooling capacities. For high and medium capacities, the numerical normalized COPs deviated less than 1% from the experimental values while for the low capacity, errors were smaller than 2.5%. With the model it is possible to locate the interface between two-phase and subcooled liquid refrigerant in the condenser for each subcooling value and subsequently calculate the heat transfer area allocated by the subcooled liquid. Figure 14 shows numerical results for the normalized COP as a function of the designated area ratio for subcooling.

Table 3: Heat transfer and pressure drop correlations

Refrigerant condensation heat transfer coefficient	Cavallini (2006)
Refrigerant boiling heat transfer coefficient	Gungor and Winterton (1976)
Refrigerant single-phase heat transfer coefficient	Turbulent: Gnielinski (1976) Laminar: Analytical solution
Air side heat transfer coefficient and friction factor for louvered fins	Chang and Wang (1997)
Two-phase refrigerant pressure drop	Friedel (1979)
Single phase refrigerant pressure drop	Friction factor from Churchill (1977)

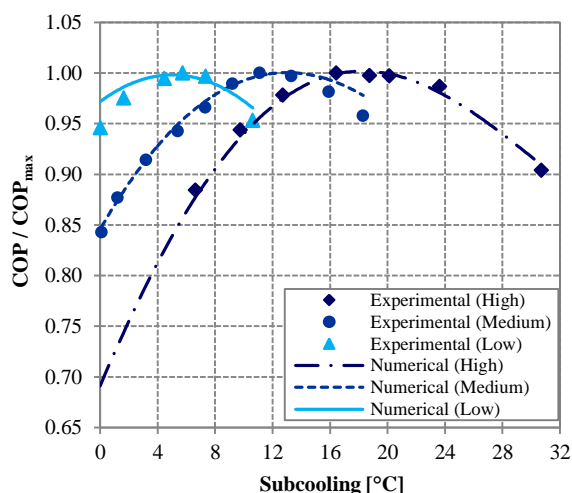


Figure 13: Experimental validation of the normalized COP predicted by the model (R1234yf)

Figure 14 indicates that, in order to maximize COP for a given cooling load, more area should be allocated for subcooling liquid in the condenser as the cooling capacity increases. These results are consistent to the analysis of the infrared images of the condenser surface (Figure 7) and to results of Figure 10 which suggested that the COP maximizing subcooling area was larger at higher cooling loads. Interestingly enough, a closer look at Figure 14 also reveals that if a subcooler pass of fixed area was to be designed, a value of 20% of the total area would yield COP to be less 2% lower than the maximum values for each of the cooling loads. Results in Figure 14 also resemble those numerically obtained by Yamanaka et al. (1997) and reproduced by Abraham et al. (2006). They showed that, for a vehicular air conditioning system, the higher the compressor speed, the larger the designated subcooling area needed to maximize COP.

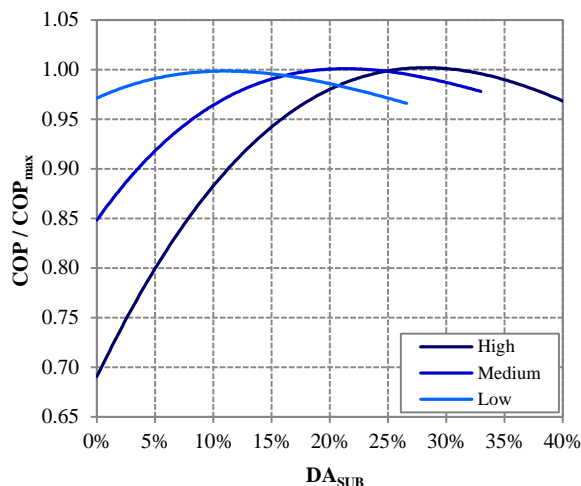


Figure 14: Numerical results for normalized COP as a function subcooling area ratio (R1234yf)

6. CONCLUSIONS

The effect of the air-refrigerant temperature difference in the condenser on the COP improvements from condenser subcooling was experimentally investigated for R134a and R1234yf in a vehicular air-conditioning system but authors believe that results can be fully extrapolated to other applications. The results indicated that the larger the air-refrigerant temperature difference, due to large cooling capacity for a given condenser size, the higher the COP maximizing subcooling and the maximum COP improvement from subcooling in condenser. For R1234yf, as the temperature difference in the condenser increased from 12°C to 29°C, the COP maximizing subcooling increased from 6°C to 16°C and the COP gains, from 6% to 44%. For R134a, COP gains ranged from 3% to 20% (half of those for R1234yf) as temperature difference in the condenser varied from 11°C to 27°C. It has been concluded that applications or operating conditions in which the size of the condenser relative to its heat transfer load is smaller will tend to benefit more from condenser subcooling.

Although experimental results for R134 demonstrated that condensers with a higher air-refrigerant temperature difference (smaller condenser size relative to its heat transfer load) will demand a larger COP maximizing subcooling to condensing area ratio, a fixed designated area ratio yielded COPs within 1.5% difference from the maximized values, within the range of cooling capacities considered (Figure 10). This was an indication that an active control of subcooling in order to maximize COP (in a non-designated area) may not be worth it. Numerical results from an experimentally validated model confirmed these findings.

With the possession of a unique set of microchannel condensers, an experimental comparison between subcooling generated in NDA (non-designated area) and DA (designated area) of the condenser revealed that both configurations yield similar values of maximum COP improvement within the range of cooling capacity considered. The results suggested that the way condenser subcooling is achieved, either in a DA or a NDA, may not be important in terms of COP.

NOMENCLATURE

<i>COP</i>	coefficient of performance	(-)	Subscripts	
<i>h</i>	enthalpy	(kJ kg ⁻¹)	<i>c</i>	condenser
<i>q</i>	enthalpy difference across the evaporator	(kJ kg ⁻¹)	<i>cp</i>	compressor
<i>T</i>	temperature	(°C)	<i>e</i>	evaporator
<i>V_f</i>	face velocity	(m/s)	<i>in</i>	inlet
<i>w</i>	specific compression work	(kJ kg ⁻¹ K ⁻¹)	<i>is</i>	isentropic
<i>DA</i>	designated area	(-)	<i>max</i>	maximum
<i>NDA</i>	non-designated area	(-)	<i>out</i>	outlet
			<i>sat</i>	saturation
			<i>sub</i>	subcooling

REFERENCES

- Abraham, G. S., Ravikumar, A. S., Shah, R. K., 2006. Design considerations for an integral-receiver dryer condenser, *In: SAE World Congress and Exhibition*, Detroit, MI, USA, paper 2006-01-0725.
- Choi, J. M., Kim, Y. C., 2002. The effects of improper refrigerant charge on the performance of a heat pump with an electronic expansion valve and capillary tube, *Energy* 27, 391-404
- Corberan, J.M., Martinez, I.O., Gonzalves, J., 2008. Charge optimisation study of a reversible water-to-water propane heat pump, *International Journal of Refrigeration* 31, 716-726
- EES, 2007. Engineering Equation Solver. Academic Professional Version 7.934-3D, *F-Chart Software*, Middleton, WI, USA.
- Farzad, M., O'NEAL, D. L., 1993. Influence of the expansion device on air conditioner system performance characteristics under a range of charging conditions, *ASHRAE Transactions* 99(2), 388-393
- Pomme, V., 1999. Improved Automotive A/C Systems Using a New Forced Subcooling Technique. *SAE International Congress & Exposition*, Detroit, MI paper 1999-01-1192
- Pottker, G., Hrnjak, P. S., 2012. Effect of Condenser Subcooling in Vapor Compressions Systems: Experimental and Numerical Investigation. *In: Proceedings of the 2012 International Refrigeration and Air Conditioning Conference at Purdue*, paper 2512
- Pottker, G., Melo, M., 2007. Experimental study of the combined effect of refrigerant charge, compressor speed and expansion valve opening in a refrigeration system. *In: Proceedings of the 2007 International Congress of Refrigeration*, China.
- Ravikumar, A.S., Karwall, N., 2005. Recent developments in automotive condensers and receiver-dryer technology, *SAE 2005 World Congress & Exhibition*, paper 2005-01-1770.
- Strupp N. C., Kohler J., Lemke N. C., Tegethoff W., Kossel R. M., 2010. Energy efficient future automotive condenser systems, *2010 International Symposium on Next-generation Air Conditioning and Refrigeration Technology*, Tokyo, Japan.
- Yamanaka, Y., Matsuo, H., Tuzuki, K., Tsuboko, T., 1997, Development of Sub-cool system, *SAE Technical Paper Series*, paper 970110

ACKNOWLEDGEMENT

The authors are thankful for the support provided by the Air Conditioning and Refrigeration Center at the University of Illinois at Urbana-Champaign and by the National Counselor of Scientific and Technological Development (CNPq) of Brazil.